Int. J. Electrochem. Sci., 16 **(2021)** Article ID: 21048, doi: 10.20964/2021.04.26

International Journal of
ELECTROCHEMICAL
SCIENCE
www.electrochemsci.org

Electrochemical sensor based on Au@Pt@Au/GO Nanohybrid for acetaminophen determination

Ling Shi[1], *Yan Huang*[1], *Na Wu*[1], *Zefeng Wang*[1,*], *Junchao Tan*[2,*]

[1] Engineering Research Center for Processing and Quality Control of Local Characteristic Food and Consumer Goods of High Education in Yunnan Province, College of Science, Honghe University, Mengzi 661199, PR China
[2] Henan Kdneu International Engineering Co.,ltd
[*]E-mail: wangzefeng841006@163.com; tanc_0371@126.com

Received: 18 December 2020 / *Accepted:* 19 January 2021 / *Published:* 28 February 2021

In this study, we reported a simple method for the preparing of gold@platinum@gold (Au@Pt@Au) nanoparticles on the surface of graphene oxide (GO) nanosheets. The prepared Au@Pt@Au/GO nanohybrids were characterized by UV-vis spectra, X-ray diffraction (XRD) and Transmission electron microscopy (TEM). The Au@Pt@Au/GO based electrochemical sensor was fabricated by immobilizing the as-prepared Au@Pt@Au/GO nanohybrids onto the bare glassy carbon electrode (GCE). The resulting Au@Pt@Au/GO/GCE electrochemical sensor was proved to detect acetaminophen (ACOP). The results showed that the proposed sensor had a high catalytic activity for ACOP and exhibited good linear relationship in the range of 0.15-125.9 μM with a detection limit of 0.045 μM. The proposed method also can be used to detect the pharmaceutical samples.

Keywords: Au NPs; Pt NPs; graphene oxide; acetaminophen

1. INTRODUCTION

Acetaminophen (ACOP) had excellent curative effect on treating fever, headache, joint pain, postoperative pain. And it widely applied in treatment of influenza disease. Not only does it relieved pain but it also inhibited the secretion of glands, reduce the outflow of nasal mucus, formation [1-3]. ACOP had low toxicity when used at the recommended doses. But overdoses of ACOP may lead to the accumulation of toxic metabolites, seriously causing nausea, vomiting, sweating, abdominal pain and pallor, serious can lead to fatal nephrotoxicity and hepatoxicity, as well as even death [3-5]. Thus, it is highly necessary to find an effective and accurate method for detection of ACOP. Recently, Variety of methods had been widely applied in detection of ACOP. For example, electrochemical method [6], capillary electrophoresis-tandem mass spectrometry method [7], HPLC-MS/MS [8], and Capillary

Electrophoresis (CE) [9], et al. Among these methods, electrochemical methods had been widely used in the field of electrochemical detection because of its high sensitivity and selectivity, fast response rates, and low costs [10, 11].

It is well known that nanostructure materials had shown some advantages in electrochemical analysis due to its excellent electrochemical activity and high conductivities. Graphene nanosheets had been widely applied in electrochemical sensors and biosensing field due to it has excellent electronic conductivity, good thermal stability, and a large large specific surface area[12]. Graphene can also be used as a good substrate material to support noble metal nanoparticles. On the other hand, Pt and Au nanoparticles (NPs) with enhanced performance have been used for electroanalysis. For example, Kim's group proposed core-shell structured Au@Pt nanoparticles modified GCE, the obtained sensor exhibited higher electrocatalytic activities towards glucose oxidation [13]. Xu' group prepared GO-supported Au@Pt@Au nanocomposites which showed high electrocatalytic ability in hydrogen peroxide oxidation and reduction [14]. Sun et al reported gold and platinum NPs decorated biomass porous carbon composite. The composites modified electrode showed good electrochemical catalytic activity for the detection of baicalein [15]. These reports showed that the Au and Pt noble metal nanoparticles showed excellent electrochemical activity toward small molecules.

Inspired by this idea, we design an effective method to prepare Au@Pt@Au/GO bimetallic nanohybrids. The morphology, structure and composition of the obtained nanohybrids were characterized by TEM, HRTEM, and XRD. The obtained nanohybrids were used to fabricate electrochemical sensor. The results showed that Au@Pt@Au/GO nanocomposite exhibited attractive electrocatalytic activity toward ACOP. More importantly, the proposed sensor can successfully detect ACOP in actual samples.

2. EXPERIMENTAL

2.1. Chemicals

Graphene oxide (GO) was obtained from Nanjing JcnanoTechnology Co., Ltd (China). $HAuCl_4$, H_2PtCl_6, $AgNO_3$, and trisodium citrate were purchased from Shanghai Eybridge Chemical Technology Co., Ltd. Acetaminophen, acetic acid, phosphoric, boric acids and other reagents were obtained from Shanghai Chemical Reagent Co. Ltd (China). The pharmaceuticals were purchased from a local pharmacy. Britton-Robison (B-R) buffer solution (0.04 M in each of acetic, phosphoric and boric acids) were uesd as supporting electrolytes. Ultra-pure water which was obtained from a Milli-Q water purifying system was used for preparation of all aqueous solutions.

2.2. Peparation of Au@Pt@Au/GO nanohybrids

Au@Pt@Au/GO nanohybrids were prepared by employing literature method with minor modifications [14]. 5.0 mg GO was dispersed in 100 mL of ultra-pure water in 150 mL three-necked bottle by ultrasonication (ultrasonic power: 100W) 2.0 h to obtain a stable mixture. 500 μL of 0.05886

M $HAuCl_4$ was added into the mixture slowly and then mixture solution was heated to boiling under stirred vigorously for 30 min. The Au NPs loaded on GO (Au/GO) nanosheets were obtained. Then 6 mL of 0.00588 M $AgNO_3$ solution and 1.5 mL of 0.0388 M sodium citrate solution was dropped into the above solution, and continued to react for 1 h. In this step, the Ag/Au/GO nanocomposites were obtained by reducing Ag^+ onto the surface of Au/GO. Then 1.616 mL of 0.0193 M H_2PtCl_6 solution was added slowly. The reaction was stirred vigorously at the ambient temperatures untill the color of the solution changed into black purple. In this step, Pt/Au/GO nanoparticles were obtained via the galvanic replacement of Ag by Pt through the addition of H_2PtCl_6, the reaction was as follows: $4Ag + PtCl_6^{2-} \rightarrow Pt + 4AgCl + 2Cl^-$. The obtained Pt/Au/GO was collected by centrifugation and washed two times with ultra-pure water. The product was re-dispersed in 60 mL ultra-pure water. The obtained solution was heated to boiling under stirred vigorously. 1.6 mL of 0.0588 M $AgNO_3$ solution was added, and then 0.4 mL of 0.0388 M sodium citrate solution was added. The solution was kept reaction for 1 h under the boiling. Finally, 0.2 mL of 2.94×10^{-4} M $HAuCl_4$ solution and 0.2 mL of 0.0388 M sodium citrate solution were added simultaneously. The mixture was stirred for 30 min. The obtained nanohybrids were collected by centrifugation and washed with ultra-pure water.

2.3. Instruments

UV-vis absorption spectra were obtained on UV-vis spectrophotometer (Perkin-Elmer Lambda 900 USA). X-ray diffraction (XRD) analysis were recorded on X'Pert^3 powder diffractometer (PANAlytical Company). XPS data was carried out on K-Alpha$^+$ spectrometer (Thermo fisher Scientific) with Al Kα radiation (hν = 1486.6 eV). The morphology of obtained nanohybrids was analyzed JEM-2100 transmission electron microscope (TEM, JEOL, Japan). All electrochemical experiments were recorded on CHI660E electrochemical workstation (CHI, Shanghai). A three-electrode system was set-up including glassy carbon electrode (GCE, 3 mm diameter) or modified GCE as working electrode, a platinum wire as counter electrode and Ag/AgCl as the reference electrode, respectively.

2.4. Electrode fabrication and measuring method

The GCE was polished with alumina slurry followed by washing with ethanol and ultra-pure water. The prepared Au@Pt@Au/GO nanohybrids were dispersed in ultra-pure water and sonicating the mixture for 10 min to obtain 1 mg/mL of aqueous dispersion. 7 μL of Au@Pt@Au/GO dispersion was droped on GCE, and dried under ambient conditions. The B-R solution was used as electroanalyte solution in cyclic voltammetry (CV) and differential pulse voltammetry (DPV) measurements. And prior to electrochemical measurements the B-R solutions were purged with high-purity N_2 for 10 min.

2.5. Pharmaceutical real samples solution preparation

The Compound Paracetamol and Amantadine tablets (0.250 g/tablet) were purchased from local drugstore. The tablets were finely powdered in a mortar with pestle and dissolved in ethanol

solution bymagnetic stirring for 10 min. The obtained solution was filtered and collected. The filtrate was diluted with B-R solution (pH=5.0) to make stock solution of ACOP from the tablet.

3. RESULTS AND DISCUSSION

3.1 Characterization of the as-prepared nanohybrids

The prepared nanohybrids were characterized by UV-vis spectroscopy. Figure 1A showed the UV-vis absorption spectra of GO and Au@Pt@Au/GO. The GO (curve a) showed a strong absorption peak at about 228 nm, which are the characteristic absorption peak of π-π* transitions of the aromatic C=C band [16]. After Au@Pt@Au loaded onto the surface of GO, an obvious signal at 544 nm assigned to the dipole mode of the SPR of Au NPs was observed, which indicating that the Au@Pt@Au/GO nanohybrids had been prepared successfully. Moreover, the X-ray diffraction (XRD) was used to investigate the crystal structure of prepared nanohybrids. As shown in Figure 1B, an obvious peak centered at 10.32° was observed, corresponding to the (002) interplanar spacing of 3.36 Å [17]. The diffraction peaks at 38.29°, 44.41°, 64.42°, 77.59° and 81.72° were attributed to the (111), (200), (220), (311), and (222) planes of Au@Pt@Au. The results were almost in agreement with the diffraction standard of Au (JCDPF-04-0784) [18] and Pt (JCPDF 04-0802) [19]. These spectral results further proved that the Au@Pt@Au/GO nanohybrids were successfully obtained.

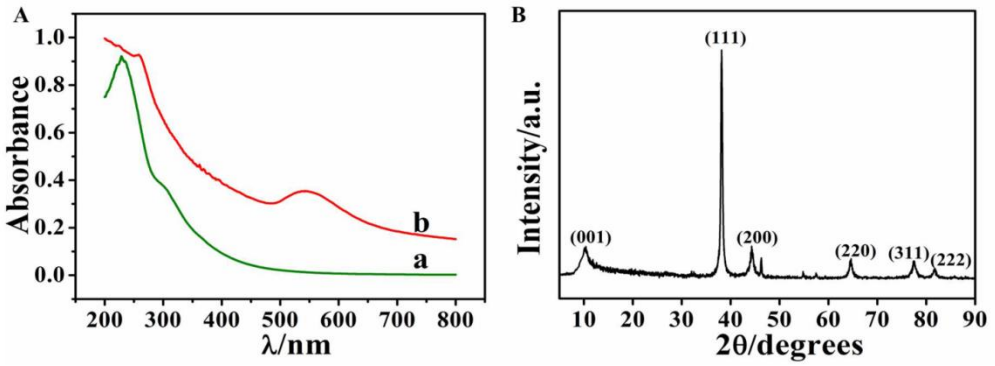

Figure 1. (A) UV-vis spectra of (a) GO, (b) Au@Pt@Au/GO nanoparticles. (B) XRD patterns of the Au@Pt@Au/GO.

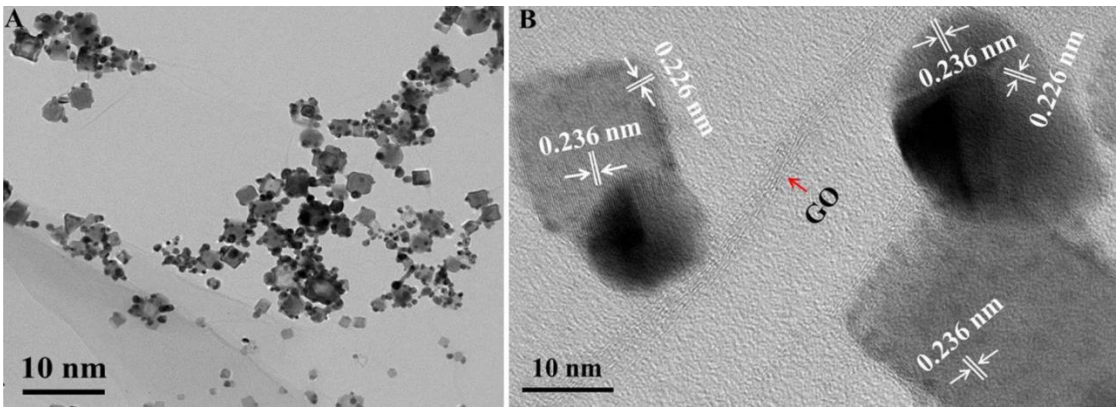

Figure 2. TEM (A) and HRTEM (B) images of Au@Pt@Au/GO nanohybrids.

The morphology of resulted Au@Pt@Au/GO nanohybrids was shown in Figure 2. The observations of TEM showed clearly that irregularly shaped Au@Pt@Au NPs were not loaded uniformly on transparent graphene surface. Small amounts of NPs were slightly aggregated due to the known chemical inertness of graphene. Furthermore, the graphene nanosheets showed crumpled silk waves-like structure and the NPs can be loaded onto both sides of these sheets. The HRTEM images showed that the lattice distances for Au NPs and Pt NPs were 0.236 nm and 0.226 nm, respectively, which can be assigned to the (111) planes of face-centered cubic (fcc) Au and Pt, respective [14]. The results further proved that the Au@Pt@Au bimetallic nanohybrids were successfully synthesized.

3.2. Cyclic voltammetry study of ACOP

The electrochemical behaviors of ACOP at Au@Pt@Au/GO/GCE have been investigated using cyclic voltammetry (CV). The CVs of ACOP at the bare GCE, GO/GCE, and the Au@Pt@Au/GO/GCE were shown in Figure 3A. The bare GCE and GO/GCE revealed a significant oxidation peak at 525 mV (curve a, b). The peak current at GO/GCE was larger than GO/GCE. It was due to the GO possessed good electrical conductivity and the electron transfer rate can be enhanced. The Au@Pt@Au/GO/GCE revealed an obvious oxidation peak at about 528 mV (cuvre c), the peak current was obviously stronger than GO/GCE. That due to the obtained Au@Pt@Au/GO/GCE had good electrical conductivity and biocompatibility can benefit to enhance the electron transfer rate for ACOP at the surface of the Au@Pt@Au/GO/GCE. Figure 3B showed the CV curves of the Au@Pt@Au/GO/GCE in the absence and presence of 300 μM ACOP. It can be observed that the modified GCE had not any redox peaks at about 528 mV in blank B-R solution (Figure 3B (a)), but when it immersed in B-R solution (pH=5.0) containing 300 μM ACOP, an obvious oxidation peaks was found at about 528 mV (Figure 3B (b)). Results indicate that the Au@Pt@Au/GO/GCE can catalyze effectively ACOP reaction on the electrode surface, and it was suitable for analysing of ACOP.

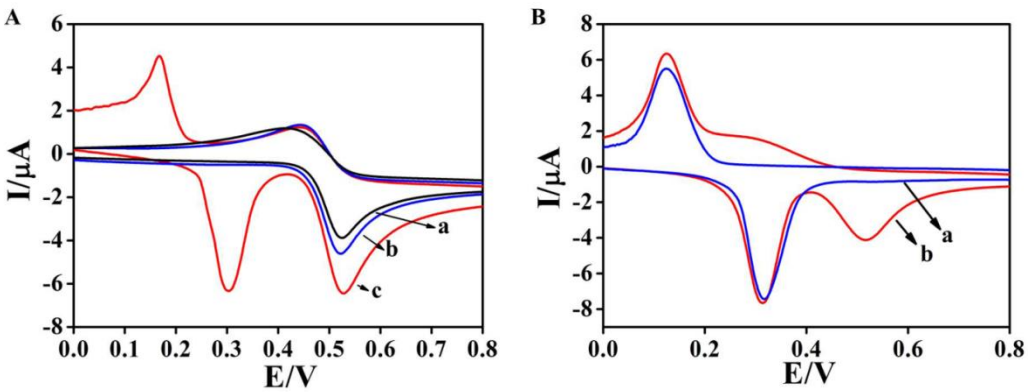

Figure 3. (A): CVs of the bare GCE (a), GO/GCE (b) and the Au@Pt@Au/GO/GCE (c) recorded in N_2-saturated B-R buffer solution (pH 5.0) containing 300 μM ACOP at a scan rate of 10 mV/s. (B): CVs of the Au@Pt@Au/GO/GCE in the absence (a) and presence (b) of 300 μM ACOP in N_2-saturated B-R buffer solution (pH 5.0) at a scan rate of 10 mV/s.

3.3. The effect of pH value

The influence of pH of the supporting electrolyte on the electrochemical behaviour of Au@Pt@Au/GO/GCE was studied. Figure 4A depicted the CV obtained in solutions containing 300 μM ACOP at different pH values in the range starting from 3.0 to 7.0. It was seen that the current response to ACOP increased with increasing pH of solutions and reached a maximum at pH 5.0. Then it was decreased with pH increasing up to 7.0. Thus, in order to get the superior detection results, all experiments were carried out in a B-R solution of pH=5.0. Furthermore, the oxidation peak potential of ACOP shifted in the negative direction as the pH increased. The peak currents were gradually increasing when pH from 3.0 to 5.0, and then peak current gradually decreased when keep increasing pH value. Thus pH=5.0 was selected as the optimum pH. Figure 4B showed the plots of anode and cathode peak potential against the pH values, respectively. A good linear relationship can be established between E_p and the solution pH. The regression equation can be expressed as E_{pa}(V) = -0.049 pH + 0.808, E_{pc}(V) = -0.055 pH + 0.73. The values of ΔE/ΔpH 49 and 55 mV were similar to the theoretical Nernstian slope. This demonstrated that the numbers of protons and electrons participating in the redox reaction of ACOP were almost equal [20, 21].

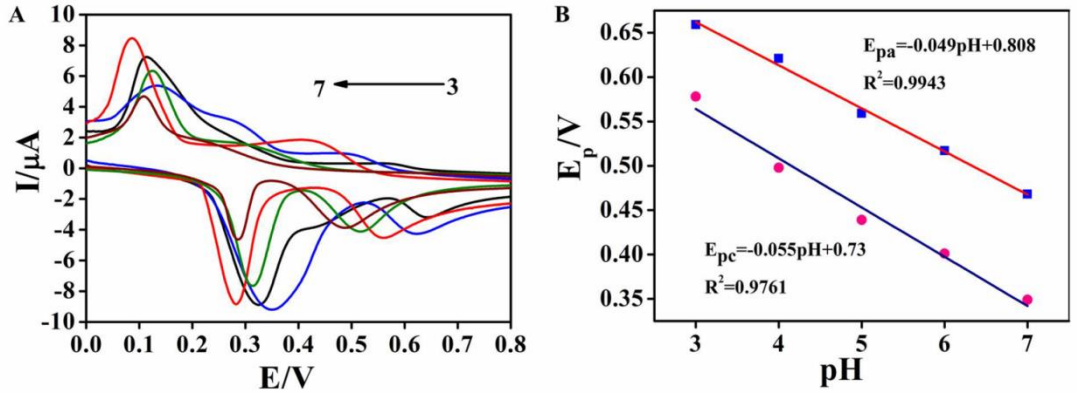

Figure 4. (A): CVs obtained at the Au@Pt@Au/GO/GCE in N_2-saturated B-R buffer solution with different pH values (3.0, 4.0, 5.0, 6.0, and 7.0) containing 300 μM ACOP at scan rate of 50 mV/s. (B): The plots of cathodic and anodic peak potential of ACOP versus pH values.

3.4. The effect of scan rate

In order to further investigate the reaction mechanisms of ACOP at Au@Pt@Au/GO/GCE, the effect of different scan rate on detection of ACOP was studied. Figure 5 showed the CVs of Au@Pt@Au/GO/GCE in N_2-saturated B-R buffer solution (pH 5.0) containing 300 μM ACOP with different scan rate. The oxidation peak currents and reduction peak currents of ACOP were seen to be linearly proportional to the square root of scan rate in the range 10-100 mV/s. The results demonstrated that the electrochemical reaction was a diffusion-controlled process [22, 23]. The corresponding equations can be obtained from Figure 5B, I_{pa} = -0.627 $\nu^{1/2}$ - 3.5591 (R^2 = 0.9785), I_{pc} = 0.2680 $\nu^{1/2}$ + 1.9370 (R^2 = 0.9520), respectively. Moreover, the oxidation peak potentials moving in the positive

direction with increasing scan rate, while the corresponding reduction peak potentials shifted to negative direction. The equations between E_p and lnν were expressed as follows: E_{pa} = 0.01448lnν+0.4916 (R^2 = 0.9484), E_{pc} = -0.02532 lnν + 0.5194 (R^2 = 0.9584), respectively. The electrochemical parameters can be estimated according to the Laviron equation [20]:

$$E_{pa} = E^{0'} + \frac{RT}{(1-\alpha)nF}\ln\upsilon \qquad \text{Eq. (A.1)}$$

$$E_{pc} = E^{0'} - \frac{RT}{\alpha nF}\ln\upsilon \qquad \text{Eq. (A.2)}$$

$$\lg k_S = \alpha\lg(1-\alpha) + (1-\alpha)\lg\alpha - \lg\frac{RT}{nF\upsilon} - \alpha(1-\alpha)\frac{nF\Delta E_p}{2.3RT} \qquad \text{Eq. (A.3)}$$

Where E_p was the peak potential, $E^{0'}$ was the formal standard potential, R indicated the universal gas constant (R=8.314 J mol^{-1} K^{-1}), T denoted the absolute temperature (T=298 K), F was the Faraday's constant (F=96485 C mol^{-1}), υ denoted the scan rate, k_s was electron transfer rate constant, n was electron transfer number, and α was charge transfer coefficient. According to Laviron equation, the slope value from the plot of anodic peak potential (E_{pa}) versus lnυ was equal to RT/(1-α)nF and the slope value from the plot of cathode peak potential (E_{pc}) versus lnυ was equal to RT/αnF, respectively. The value of n, α and k_s can be calculated were about 2, 0.36 and 0.186 s^{-1}, respectively. Hence, these results implied that the electrochemical oxidation of ACOP was two electron transfer process.

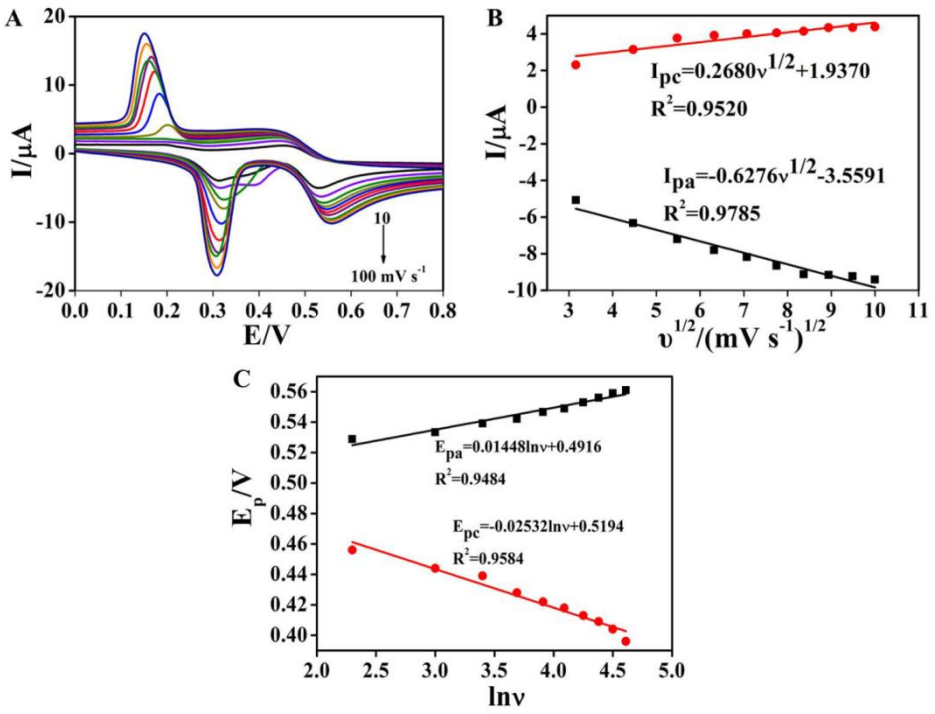

Figure 5. (A): CVs of Au@Pt@Au/GO/GCE in N_2-saturated B-R buffer solution (pH 5.0) containing 300 μM ACOP at scan rate of 10, 20, 30, 40, 50, 60, 70, 80, 90, and 100 mV/s (from inner to outer curve). (B): Linear relationship of cathodic and anodic peak current versus the square root of scan rate. (C) Plots of anodic and cathodic potentials against the lnν.

3.5. Analysis of ACOP on Au@Pt@Au/GO/GCE

The different concentrations ACOP were detected under the optimized experimental conditions on Au@Pt@Au/GO/GCE by DPV. The results were shown in Figure 6, the oxidation current were linearly increasing with vary of concentrations ACOP. The relationship between peaks current and concentration can be obtained from Figure 6B. The regression equation was I=-0.0584C-0.2052 (R^2=0.9972). The fabricated sensor displayed a linear range of 0.15-125.9 μM with the limit of detection was 0.045 μM (S/N=3). The obtained detection limit and linear range for ACOP was compared with the other research groups (Table 1). It was worth noting that the fabricated sensor revealed better results compared to other nanomaterials modified electrodes. The proposed sensor revealed a very low detection limit compared to other graphene related materials [1, 4, 21, 24, 25]. These results suggested that the synergic effect of Au NPs, Pt NPs and GO could greatly enhance analytical performance of fabricated sensor for analysis ACOP.

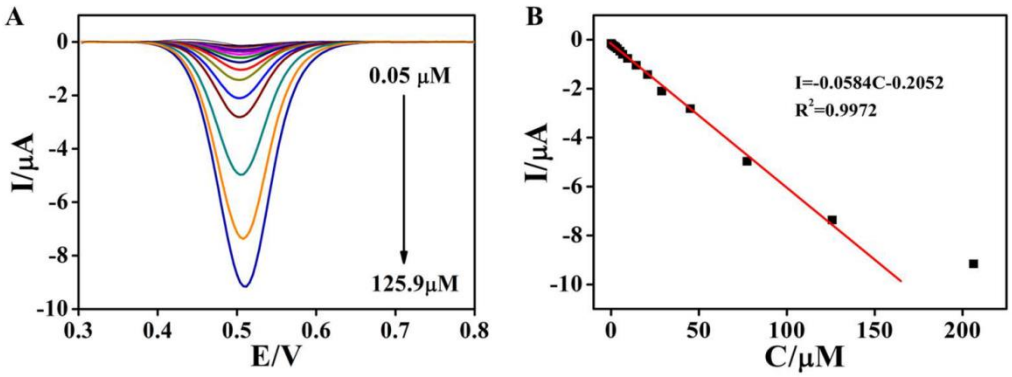

Figure 6. (A): DPVs of 0.05, 0.15, 0.74, 1.74, 2.61, 3.62, 5.11, 6.68, 9.5, 14.3, 20.8, 28.9, 45.1, 77.4, 125.9, and 206.4 μM ACOP on Au@Pt@Au/GO/GCE in N_2-saturated B-R buffer solution (pH 5.0). (B): the plot of peak current versus ACOP concentration.

Table 1. Comparison of analytical parameters for ACOP determination at different modified electrodes.

Modified GCE	Linear range/μM	Detection limit/μM	Reference
PEDOT/GO/GCE	10-60	0.57	[24]
β-CD/RGO-GCE	10-800	2.3	[25]
Pd-POMs-OMC–GCE	0.10-33.15	0.067	[21]
P-RGO/GCE	1.5-120	0.36	[4]
CoAl-OOH/rGO/GCE	0.1-30	0.058	[1]
Au@Pt@Au/GO/GCE	0.15-125.9	0.045	This work

3.6. Selectivity, reproducibility, and stability of fabricated sensor

In order to evaluate the selectivity of Au@Pt@Au/GO/GCE toward ACOP, foreign species were added into B-R solution (pH=5.0) when presence of ACOP. Consequently, 2 mM of ascorbic

acid, glucose, $CaCl_2$, KCl, and NaCl, had no influence on the detection of 300 μM ACOP. The results showed that fabricated sensor had excellent selective for detection of ACOP. The reproducibility of Au@Pt@Au/GO/GCE was also investigated for the determination of 300 μM ACOP by five Au@Pt@Au/GO/GCEs fabricated using the same procedure. The RSD value was 3.1%, demonstrating the fabricated sensor possessed good reproducibility. The stability of proposed sensor was also evaluated by detecting ACOP at different times with same sensor. The responses were monitored every 6 days in B-R solution containing 300 μM ACOP. It was noted that the current response of Au@Pt@Au/GO/GCE was almost no changed. These results revealed that the fabricated Au@Pt@Au/GO/GCE sensor have excellent selectivity, stability and reproducibility.

The fabricated Au@Pt@Au/GO/GCE sensor was used to detect ACOP in Compound Paracetamol and Amantadine tablets. The detection of sample was carried out using DPV under optimized experimental conditions. The 5 μL stock solution made from the ACOP tablets were added into N_2-saturated B-R buffer solution (pH 5.0). As shown in Table 2, the content of ACOP in the tablet was 246.9 mg/tablet, which was in good accordance with the declared value. These results show that the fabricated Au@Pt@Au/GO/GCE sensor was suitable for the determination of actual samples.

Table 2. Determination of ACOP in Compound Paracetamol and Amantadine tablets.

sample	Declared (mg/tablet)	Average (mg/tablet)	RSD (%)
1	250	243	1.8
2	250	253	2.5
3	250	245	2.1
average	250	247	

4. CONCLUSION

In this work, Au@Pt@Au Nanoparticles on graphene oxide nanosheets (Au@Pt@Au/GO) were obtained using a simple method. The obtained nanohybrids were used to fabricate sensor for electrochemical detection of ACOP. The results indicated that the Au@Pt@Au/GO/GCE had excellent electrocatalytic activity toward the redox of ACOP. The linear range was 0.15-125.9 μM with the detection limits of 0.045 μM. Moreover, the obtained sensor had excellent selectivity, reproducibility, and stability, and can be used to detect actual samples.

ACKNOWLEDGMENTS
This work was supported by the Scientific Research Funddation of Yunnan Education Department (Grand No. 2020J0672), National Natural Science Foundation of China (Grand No. 21665008), Junior High School Academic and Reserve Program of Yunnan Province (Grand No. 2018HB005), the Yunnan education department of Scientific Research Foundation (Grand No. 2018JS478), the PhD Start-up Fund of Honghe University (Grand No. XJ16B04), Young Academic Reserve Program of Honghe University (Grand No. 2016HB0401).

References

1. Cheng Ke Wu, Jing Li, Xiao Ya Liu, Hui Jie Zhang, Rui Feng Li, Gong Ke Wang, Zhen Hui Wang, Q. M. Li， and En Bo Shang Guan, *Materials Science and Engineering: C*, 119 (2021) 111557.
2. W. C. Liang, L. L. Liu, Y. G. Li, H. L. Ren, T. T. Zhu, Y. W. Xu and B. C. Ye, *J. Electroanal. Chem.*, 855 (2019) 113495.
3. F. Li, R. X. Li, Y. Feng, T. Gong, M. Z. Zhang, L. Wang, T. J. Meng, H. X. Jia, H. Wang and Y. F. Zhang, *Mater. Sci. Eng.*, C, 95 (2019) 78.
4. X. Zhang, K. P. Wang, L. N. Zhang, Y. C. Zhang and L. Shen, *Anal. Chim. Acta*, 1036 (2018) 26.
5. S. M. Yu, H. F. Li, G. G. Li, L. T. Niu, W. L. Liu and X. Di, *Talanta*, 184 (2018) 244.
6. Mehrnoosh Sadeghi and M. Shabani-Nooshabadi, *Prog. Org. Coat.*, 151 (2021) 106100.
7. Marie Lecoeur, Guy Rabenirina, Nadège Schifano, Pascal Odou, Sabine Ethgen, Gilles Lebuffe and Catherine Foulon, *Talanta*, 205 (2019) 120108.
8. Matt Barfield, Neil Spooner, Rakesh Lad, Simon Parry and S. Fowles, *J. Chromatogr. B*, 870 (2008) 32.
9. F.Y. He, A.L. Liu and X.H. Xia, *Anal. Biochem*., 379 (2004) 1062.
10. M. Arvand, A. Shabani and M. Sayyar Ardaki, *Food Anal. Methods*, 10 (2017) 2332.
11. M. Arvand and S. Hemmati, *Sensors Actuators B Chem.* , 238 (2017) 346.
12. Z. F. Wang, G. Z. Gou, L. Shi, J. Yang, C. Xu, L. Zhang, A. P. Fan and Y. Min, *J. Appl. Polym. Sci.*, (2018) 46720.
13. Kyubin Shim, Won-Chul Lee, Min-Sik Park, Mohammed Shahabuddin, Yusuke Yamauchi, Md Shahriar A. Hossain, Yoon Bo Shimb and J. H. Ki, *Sensors & Actuators: B. Chemical*, 278 (2019) 88.
14. X. R. Li, M. C. Xu, H. Y. Chen and J. J. Xu, *Journal of materials chemistry. B*, 3 (2015) 4355.
15. Hui Cheng, Wen Ju Weng, Hui Xie, Juan Liu, Gui LIng Luo, Shao Mei Huang, Wei Sun and Guang Jiu Li, *Microchem. J.*, 154 (2020) 104602.
16. A. A. Vernekar and G. Mugesh, *Chem. Eur. J.*, 18 (2012) 15122.
17. Virendra V. Singh , Garima Gupta , Anirudh Batra , Anil K. Nigam , Mannan Boopathi , Pranav K. Gutch , Brajesh K. Tripathi , Anchal Srivastava , Merwyn Samuel , Gauri S. Agarwal , Beer Singh and R. Vijayaraghavan, *Adv. Funct. Mater.*, 22 (2012) 2352.
18. R. J. Liu, S. W. Li, X. L. Yu, G. J. Zhang, S. J. Zhang, J. N. Yao, B. Keita, L. Nadjo and L. J. Zhi, *Small*, 8 (2012) 1398.
19. B. Y. Xia, W. T. Ng, H. B. Wu, X. Wang and X. W. Lou, *Angew. Chem., Int. Ed*., 51 (2012) 7213.
20. K. Sheng, L. Wang, H. C. Li, L. Zou and B. X. Ye, *Talanta*, 164 (2017) 249.
21. X. Y. Kong, Y. Y. Wang, Q. Q. Zhang, T. R. Zhang, Q. Q. Teng, L. Wang, H. Wang and Y. F. Zhang, *J. Colloid Interface Sci.*, 505 (2017) 615.
22. L. Shi, Z. F. Wang, N. Wu, G. Z. Gou, X. L. Chen, G. M. Yang and W. Liu, *Int. J. Electrochem. Sci.*, 15 (2020) 3660.
23. L. Shi, Z. F. Wang, N. Wu, X. L. Chen, G. M. Yang and W. Liu, *Int. J. Electrochem. Sci.*, Vol., 15 (2020) 3204
24. W. M. Si, W. Lei, Z. Han, Y. H. Zhang, Q. L. Hao and M. Z. Xia, *Sensors Actuators B: Chem.*, 193 (2014) 823.
25. L. Fu, G. S. Lai and A. M. Yu, *RSC Adv.*, 5 (2015) 76973.